Microstructure and annealing behaviour of cold-drawn isotactic polypropylene

J. PETERMANN*, J. M. SCHULTZ
Department of Chemical Engineering, University of Delaware, Newark, Delaware 19711, USA

Isotactic polypropylene tensile bars were cold-drawn at room temperature and subsequently annealed for various times at temperatures ranging from 50 to 155° C. The material was examined at room temperature in the as-drawn state at several stages of annealing. SAXS, density and mechanical loss data were obtained. Furthermore, thin films were cast. These films were drawn at −196° C and subsequently examined in the electron microscope at −120° C and at higher annealing temperatures. SAXS results for lower temperature annealing showed increases in the intensity of the small-angle Bragg hump with no change in position. High temperature annealing produced a very large intensity increase. In no case did the density of the material show a large increase. Electron microscopy indicated a microstructureless material in the as-drawn state. Annealing at low temperatures produced a fibrous morphology with no observable density modulation in the draw direction. High temperature annealing produced a lamellar microstructure with "normal", stepwise density modulation. Dynamical mechanical loss curves exhibited no or little β relaxation, except after high temperature annealing. On the basis of these observations, a microstructural model is proposed. The model suggests a very highly defective crystal or paracrystal in the as-drawn state. Low temperature annealing promotes a fibrillar, fringed micellar morphology, in which "crystalline" and "amorphous" regions are not clearly delineated. At higher annealing temperatures, a lamellar, two-phase microstructure is produced.

1. Introduction

The structure of semicrystalline polymers in the oriented state has been emphasized by numerous authors [1–13]. Depending on crystallization conditions (i.e., from oriented melts or cold-drawn material) different models have been proposed. Basically three different morphologies are used to describe the oriented structure: (i) extended-chain crystals with lamellar overgrowths [8], (ii) a stacking sequence of oriented crystal lamellae [10], and (iii) a fringed-micelle type [1]. All the other models are combinations of those morphologies. It is the purpose of this work to investigate the structure of cold-drawn isotactic polypropylene and its change during annealing. The structure was explored using both microscopic (transmission electron microscopy, election diffraction, and small-angle X-ray diffraction), and macroscopic (mechanical loss and density measurements) methods. It will be shown that the cold stretched state is best described by an oriented micelle and that an annealing treatment changes the morphology into a lamellar type. The transformation occurs by a *gradual* reapportionment of density between more-dense and less-dense regions. The transformation process may resemble that of spinodal decomposition.

2. Experimental

The material used for all investigations, except electron microscopy was Hercules Pro-fax High Crystallinity moulding grade isotactic poly-

*On leave from Universität des Saarlandes, 66 Saarbrücken, West Germany.

propylene. The material used for electron microscopy was Hostalen PPN, an isotactic polypropylene supplied by Farbwerke Höchst AG. Specimens were compression moulded as 3 mm thick sheets and water quenched. The as-quenched material was transparent and unoriented. Pinole X-ray photographs show a strong monoclinic (α) pattern with only a relatively weak amorphous halo. Presumably this material is composed of poorly-developed spherulite cores; well-developed spherulites would scatter light and the material would not be transparent. Tensile specimens were milled from the sheets and drawn in an Instron machine at room temperature with a deformation rate of 10^{-5} sec^{-1}. The necked regions, which were also optically transparent, were cut into strips of 4 cm length and 0.5 cm width.

Most of the small angle X-ray scattering (SAXS) work was performed using a Kratky camera with FeKα radiation. However, a few point-collimated curves were obtained using the Oak Ridge 10-meter SAXS instrument, which utilizes a 2-dimensional position-sensitive detector. For the mechanical loss measurements, a Rheo-Vibron was used with a frequency of 11 Hz and a heating rate of 1° C min^{-1}. The density was determined in a gravity column, using toluene and carbon tetrachloride as liquids.

For transmission electron microscopy (TEM) and electron diffraction, samples were prepared as follows. A droplet of a 0.1% solution of the polymer in *o*-xylene was deposited on the surface of hot orthophosphoric acid (190° C). When the solvent evaporated, the polymer spread out into a thin molten layer, which was then removed and quenched in water. Electron diffraction patterns from this as-quenched material (see Fig. 5a) were essentially identical with the X-ray pinole patterns from the thicker quenched sheet; the crystalline regions are in the α (monoclinic) modification and are of statistically random orientation. Pieces of the quenched film were collected on the electron microscope grids. Drawing was performed at liquid nitrogen temperature (-196° C) on the grids in the straining device of the electron microscope. As the film adheres firmly to the bars of the grids, the film deforms approximately the same amount as the microscope grids. The deformed grids were
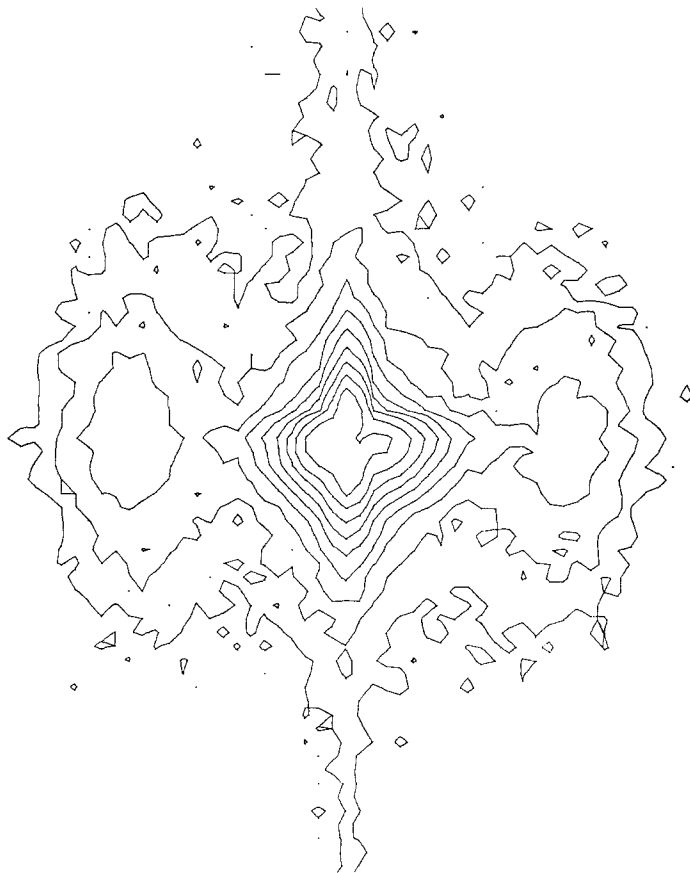

Figure 1 Pinhole-collimated SAXS pattern of material drawn at room temperature and subsequently annealed 30 sec at 155° C.
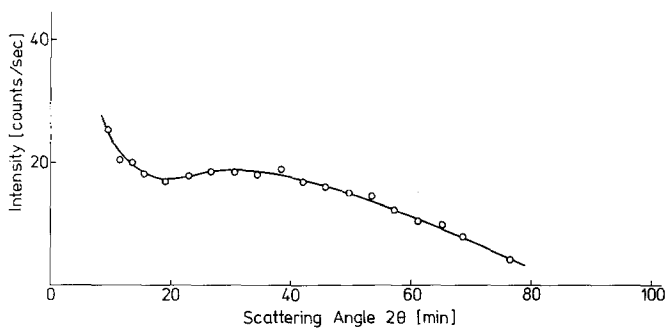
subsequently remounted from the straining device to the cooling device. During this procedure the highest temperature the sample obtained was −120° C. The electron microscope used was a JEM 200 A, operated at 100 kV. For imaging, the defocusing method [12] was applied.

3. Results

(1) Small-angle X-ray scattering (SAXS): Room temperature SAXS results were obtained from material which had undergone different heat treatment at several temperatures, following room temperature drawing. These results provide information regarding the recovery of relatively long-range density fluctuations during the heat treatment . Fig. 1 shows a point-collimated SAXS curve for a piece which had been annealed at 155° C for 30 sec (our most severe anneal). The lamellar orientation is very high. Less severe annealing also produced oriented SAXS patterns; but of much lower intensity. Fig. 2 is a slit-smeared SAXS curve from the as-quenched material. A very broad hump is observed, indicative of a broad distribution of lamellar spacings. A maximum at about 30′ is seen. Fig. 3 shows slit-smeared SAXS curves for drawn and annealed material. (The effect of de-smearing would be to sharpen the observed

humps and to move them to a slightly higher angle).The as-drawn material showed no or only a very poorly developed SAXS hump and very low intensity. During annealing at 65° C, a small hump in the SAXS trace occurred. The angular position of the hump occurred at a much higher angle (∼ 55′) than that of the as-quenched material, indicating a complete disruption of the original lamellar stacking and the generation of a new stacking sequence. The position of the hump remained nearly constant with annealing time. The height of the hump increased continuously for annealing times of up to 12 hours and remained approximately constant for longer annealing times. Annealing at 130° C resulted in a much higher peak, with a periodicity similar to that of the original sheet.

(2) Electron diffraction and microscopy: Electron diffraction studies were also made. Such results are sensitive to the nearest neighbour environments and thus form an important complement to SAXS and other measurements, which are sensitive to longer range structure. Thin films of isotactic polypropylene can be deformed without rupture at temperatures as low as −196° C. The appearance of the deformed regions is the same as in samples drawn at high temperatures.
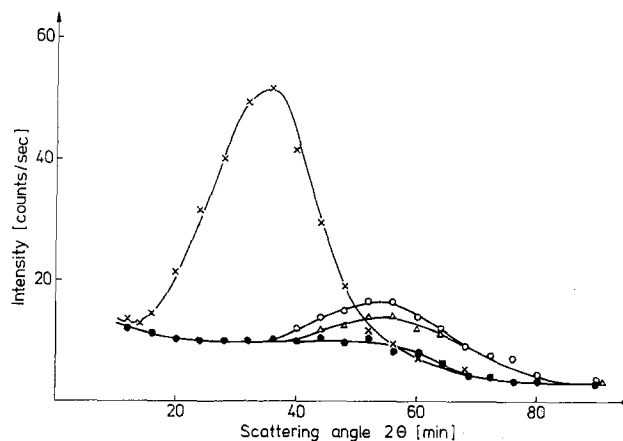

Figure 3 Slit-collimated SAXS curves of the cold-drawn and annealed samples: as-drawn (·), $\frac{1}{2}$ h at 65° C (Δ), 12 h at 65° C (o), $\frac{1}{2}$ h at 130° C (×).
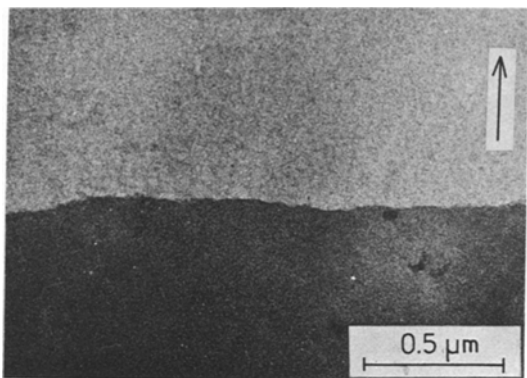
Figure 4 Transmission electron micrograph of a cold-drawn film. The brighter area is the necked region. The arrow indicates the drawing direction.

In Fig. 4, a deformed region of a sample, drawn at −196° C, can be seen. Fig. 5b shows the diffraction pattern of this region. The diffraction was obtained at −120° C (in the cooling device used, investigation at lower temperatures was not possible). Rather diffuse crystalline reflections can be

seen. After annealing the same sample at 65° C, the diffraction patterns became sharper (Figs. 5c and d) and no further significant change in the diffraction patterns was observed on annealing at 130° C (Fig. 5e).

In order to obtain further information about the structure of the drawn regions, samples first stretched at −196° C and then annealed at different temperatures were deformed, at room temperature, perpendicular to the previous drawing direction. In this way, it is possible to examine both the lamellar microstructure and whatever fibrillar superstructure may be present. In Figs. 7a and b electron micrographs of necked regions can be seen. In the sample annealed at 65° C, the necked region showed a fibrillar network with the fibrils being about 40 Å in width. The sample annealed for $\frac{1}{2}$ h at 130° C showed plane fracture parallel to the molecular direction. Furthermore, no superstructure in the non-annealed, uniaxially-drawn region is visible, while the annealed sample ($\frac{1}{2}$ h at 130° C) showed a lamellar structure per-
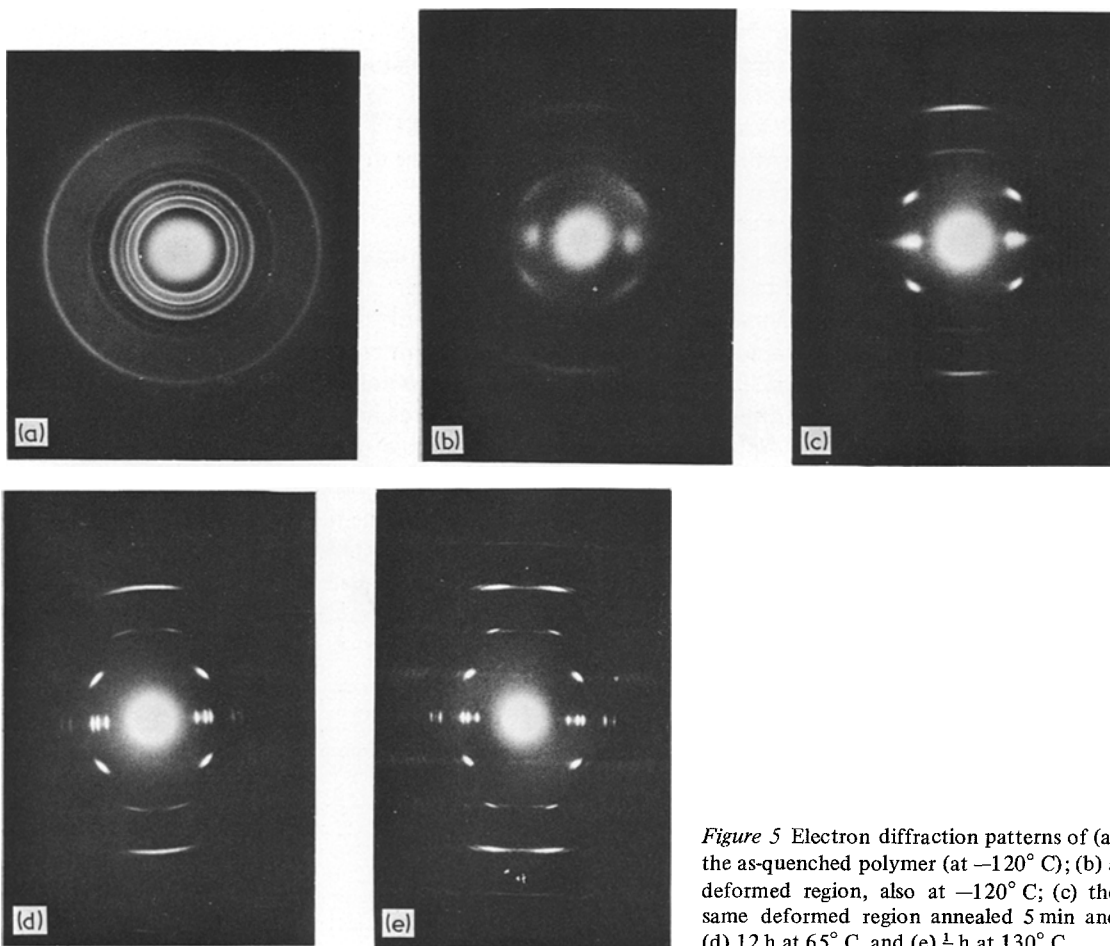

Figure 5 Electron diffraction patterns of (a) the as-quenched polymer (at −120° C); (b) a deformed region, also at −120° C; (c) the same deformed region annealed 5 min and (d) 12 h at 65° C, and (e) $\frac{1}{2}$ h at 130° C.
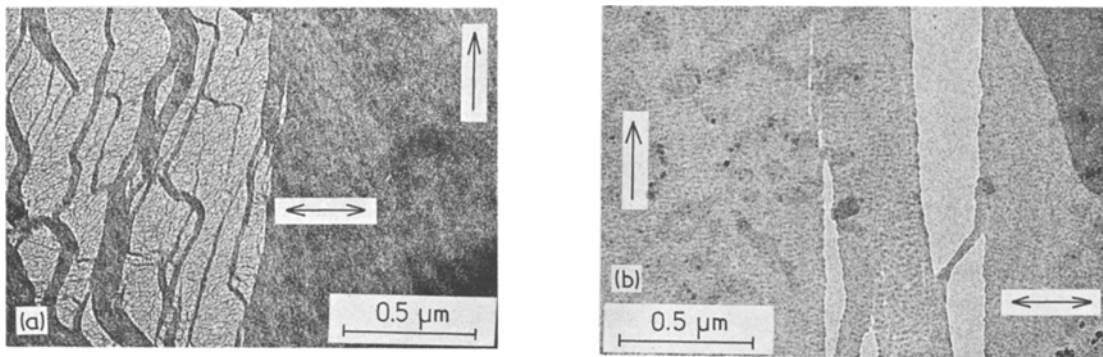
2191

Figure 6 Transmission electron micrographs of cold-drawn films. The arrow indicates the drawing direction. After cold drawing, the films were annealed (a) ½ h at 65° C and (b) ½ h at 130° C. Subsequently, the films were strained perpendicular to the previous drawing direction (indicated by a double arrow).

pendicular to the drawing direction with a lamellar spacing of about 190 Å. The contrast was obtained by the phase-contrast method, without staining [12].

(3) Mechanical loss measurements: As is shown in the next section, the above results appear to arise from variations in the nature of the "amorphous" regions. In this context, the β loss peak was also examined. The character of this peak provides a measure of molecular motion in the "amorphous" domains. Mechanical loss tangents are shown in Fig. 7. No loss peak for the glass transition temperature (which is between $-5°$ C and 15° C [13] for isotactic polypropylene) appeared in the cold-stretched sample. Annealing this sample at 65° C shifted the loss tangents to somewhat higher values in the temperature range between -20 and 50° C without changing the curve significantly. After an annealing treatment for ½ h at 130° C a loss peak at 10° C appeared, corresponding to the glass transition temperature of polypropylene. Thus the amorphous regions of

the drawn material, even after annealing at 65° C, show a greatly reduced segmental material, relative to virgin material deformed and then annealed at much higher temperature.

(4) Density measurements: Together with SAXS results, macroscopic density measurements can provide information on the apportionment mass between different regions of the material (see next section). The as-drawn material exhibited a room temperature density of 0.889 g cm^{-3}. After annealing at 65° C, the density increased only slightly, while after annealing at 130° C a strong increase in the density was observed (see Table I).

4. Discussion

The microstructure of oriented states is a fabric of many threads: the arrangement, size, shape, and orientation of the crystalline regions; the size, shape, and orientation of the noncrystalline regions; the conformation of molecules on the two regions; the defect state of the crystalline regions; and the nature of the interfaces between crystalline and noncrystalline domains. These all act together to define the mechanical behaviour of the material. The details of this microstructure must depend on the method by which the orientation was generated [9, 10, 14–17] (e.g., by crystalliz-
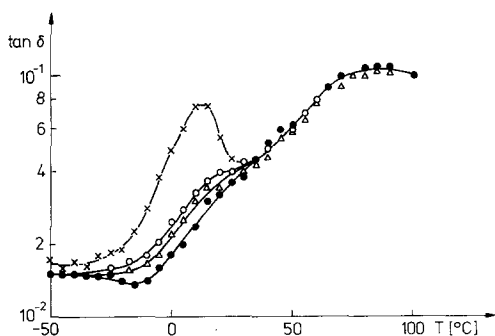

Figure 7 Mechanical loss tangents against temperature: (·) as-drawn, (Δ) annealed for 30 min at 65° C, (○) annealed for 12 h at 65° C, (×) annealed for ½ h at 130° C.

TABLE I

Annealing procedure	Sample density (g cm^{-3})
After stretching at room temperature	
1 min at 65° C	0.889
10 min at 65° C	0.890
100 min at 65° C	0.897
1 week at 65° C	0.893
30 min at 130° C	0.904

ation from a deformed melt or glass or by deformation of solid semicrystalline material). In this paper, the structure after cold-drawing and after subsequent annealing treatments is studied.

There are two principal models which describe the microstructure of cold-drawn semicrystalline polymers. In one model, a defect crystal with many chain folds randomly incorporated in the crystalline lattice is proposed. The accumulation of these chain folds during annealing leads to a lamellar structure [9]. In the other model, an oriented fringed micelle structure, where one molecule penetrates several crystallites [3] is proposed.

From the results obtained in this work, we are able to suggest the following:

(a) The material at $-120°$ C, following drawing at $-196°$ C, can be described as either a very defective crystal or paracrystal.

(b) The crystalline regions formed during annealing at relatively low temperatures ($\simeq 65°$ C) are more micellar than lamellar.

(c) At relatively low annealing temperatures, the material cannot be described as an ideal two-phase composite of "pure" crystalline and amorphous phases.

(d) Annealing at high temperature (above $130°$ C) transforms the material from a micellar into a lamellar microstructure.

The evidence for the above is now described:

(a) The nature of material stretched at $-196°$ C and "annealed" at $-120°$ C can be inferred from the combined electron diffraction and macroscopic density results. In the as-drawn state, the meridional electron diffraction spots are very diffuse both parallel and perpendicular to the direction of drawing. We will call particular attention to the broadening component which lies parallel to the drawing direction. The spots gradually sharpen as the annealing time at $65°$ C is increased. The initial broadening could be due to either particle size or to defect effects. The density results permit us to discriminate between these two cases. Were crystals to grow by a significant amount during annealing, this growth would occur at the expense of the amorphous material, and a corresponding increase in the macroscopic density should occur. The density increase over one week at $65°$ C corresponds, however, to only approximately 10% increase in crystallinity, using accepted values [18] for the densities of the two phases. This is not enough to account for the disappearance of the chain parallel component of the electron diffrac-

tion spot broadening. From this it must be concluded that the line broadening of the wide-angle electron diffraction patterns originates from lattice distortion rather than crystallite size.

Natta has termed the crystal structure of the cold-stretched isotactic polypropylene, as well as that of material rapidly quenched from the melt, "smetic" [19], meaning, in this case, that right- and left-handed helices are arranged randomly, to give a pseudohexagonal structure, whereas in the normal monoclinic unit cell, the helices are regularly arranged with respect to one another [20]. On the other hand, Miller has described this structure as "paracrystalline" [21], in the sense postulated by Hosemann. From our results, no decision can be made for either model.

(b) In the fringed-micelle crystal a molecule traverses the crystal without folding back into the same crystal. Here the crystalline regions can be regarded as junctions acting as stiffeners within an otherwise amorphous network of disordered chains [22]. While crystallizing fringed micelle crystals from the melt is unlikely for several reasons, the formation of a fringed micelle is most favourable for the crystallization of a cold-stretched polycrystal [23].

The fractured part in the cold-stretched region (Fig. 6a), resulting from drawing perpendicular to the stretch direction, illustrates both the small lateral dimensions of the "crystallites" and the strong draw-direction bonding between them. These are both characterizing features of the fringed micelle.

(c) The most serious arguments against the fringed micelle are its high surface energy [24] and the strain generated at the crystalline/amorphous interface by molecules which run from the crystalline into the amorphous phase [19].

The crystallization process at relatively low temperatures cannot be influenced by long range diffusion on the molecular segments. A metastable crystal (with higher surface energy) is thus not unlikely. Furthermore, recent work on polyethylene terephthalate has shown that the semicrystalline structure after cold stretching cannot be described by a two-phase model with a sharp interface between the crystalline and amorphous regions [25].

Examining the SAXS results (Fig. 3) in combination with the overall density measurements described in this work, the same conclusion must

be reached. While the overall density is little changed during annealing at 65° C (Table I), the integrated intensity of the SAXS hump increases markedly with time. A well-known equation of SAXS states that the intensity integrated over reciprocal space is [26],

$$\int I(s)\,\mathrm{d}v_s = K_1 \phi_c (1 - \phi_c)(\rho_c - \rho_a)^2 \quad (2)$$

Where K_1 is a constant, ρ_c and ρ_a are the densities of the amorphous and crystalline phases, and ϕ_c is the mass fraction of the crystalline regions. This law is valid only for a two-phase mixture with sharp interfaces. Using reported values of 0.9323 and 0.8535 g cm^{-3} for the crystalline and amorphous phases [18], the product ϕ_c $(1 - \phi_c)$ varies only from 0.224 in the as-drawn material to 0.229 in the most severely annealed material. The increase in integrated SAXS intensity can, in that case, be due either to large changes in $(\rho_c - \rho_a)^2 = (\Delta\rho)^2$ or to a failure of the sharply-bounded two-phase model on which Equation 2 is based. Either an amorphous—crystalline transition layer, which sharpens with annealing, or a recovery process, where vacancies (free chain ends) diffuse from the crystalline into the amorphous zones, can explain the SAXS and density measurements. The diffusion of vacancies into the amorphous zones will reduce the stress in the interfaces of micelles and will either increase the crystalline density and decrease the amorphous density, or will change the width of the transition layer. Fischer et al. [25] came to similar conclusions, with the difference that they interpreted their results in a lamellar structure.

Fig. 8 is a model of the density changes which may occur upon relatively low temperature annealing. The model shows a gradual continuous periodic modulation of density. The amplitude of the modulation increases with annealing time. In this model, the overall density changes little with time, while the density modulation increases. This model of transformation is structurally similar to a spinodal decomposition. In both cases, a discrete-phase microstructure may develop as a late stage of the transformation.

(d) In Fig. 6c, the lamellar morphology of the cold-stretched and subsequently annealed part of the sample can be clearly resolved. Comparing the mechanical loss data (Fig. 7), the SAXS curves (Fig. 3), and the fracture behaviour (Fig. 6) from samples annealed at 65° C and 130° C, respectively, a remarkable difference is observed. Not only the shape and size of the crystallites is changed. More pronounced is the change occurring in the amorphous phase, as reflected by the mechanical loss measurements. No loss peak at the glass transition temperature is detected in samples annealed at 65° C, but a well-developed T_g peak is observed in samples annealed at 130° C. Even if one takes the change of ϕ_c (Equation 2) into account, the increase of the integrated intensity of the SAXS curves has to be attributed mainly to an increase of $\Delta\rho = \rho_c - \rho_a$. The conclusion one reaches is that the micellar morphology, characterized by small crystallites interconnected by a large number of tie chains, transforms into a lamellar morphology with many folds and free chain ends in the amorphous phase. This microstructural change is seen directly in the electron micrographs in Fig. 6. There we observe fine fibrillation after lower temperature heat treatment, whereas after 130° C annealing one observes no fibrillation, but rather very broad crystallites.
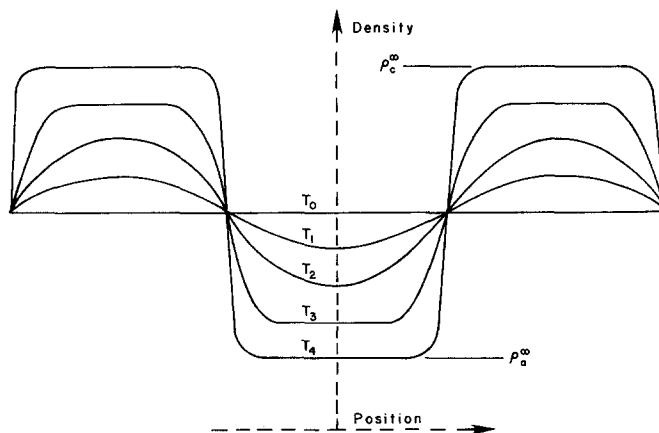

Figure 8 Model for density modulation along the draw direction. Density curves correspond to isochronal annealing at various temperatures T_i $(T_4 > T_3 > T_2 > T_1 > T_0$ = room temperature).

A comparison of SAXS and electron diffraction results after 65° C and 130° C anneals gives further evidence toward such a micellar–chain folding transformation. We have already seen that the large SAXS intensity increase between specimens treated at 65 and 130° C relates to an increase in $\rho_c - \rho_a$. But there is no apparent change in the electron diffraction spot broadening or position between these two treatments. Thus there can be no significant change in the *crystal* parameters in these two cases and the change in $\rho_c - \rho_a$ must here be interpreted as a change in ρ_a only. The driving force for chain folding is the release of strain, due to too high density of chains leading from crystal to amorphous regions. Thus a decrease of ρ_a must accompany a micelle–chain folding transition, and that is what is observed.

A similar transition has been reported by Peterlin *et al.* [6, 27] for isotactic polypropylene and linear polyethylene by means of permeability, infra-red dichroism, SAXS and electron microscopy. They interpret the changes in physical properties as a transition from a fibrillar into a lamellar structure, but do not describe the

microfibrils as micellar. Similar results have been obtained by Yeh *et al.* on isotactic polystyrene and polyethylene terephtalate [28, 29].

Numerous models have been proposed for the morphological structure in the oriented state and it is evident from mechanical properties, permeability and other methods [14] that the orientation of the molecules, as revealed by wide-angle X-ray scattering (WAXS), cannot describe uniquely the structure of fibrous materials. This means that the arrangement and size of the oriented crystallites, the configuration of the molecules in the amorphous state, the interfaces between crystalline and amorphous areas, and crystal lattice distortions are of crucial importance for mechanical properties. Furthermore, the orientation process, whether by crystallization from a melt or from a glassy state, or by different deformation mechanisms will lead to a different oriented structure, [8, 10, 14–17].

In this paper, the structure of the cold-drawn isotactic polypropylene and its change with annealing according to new results is shown schematically in Fig. 9. It remains a matter for further
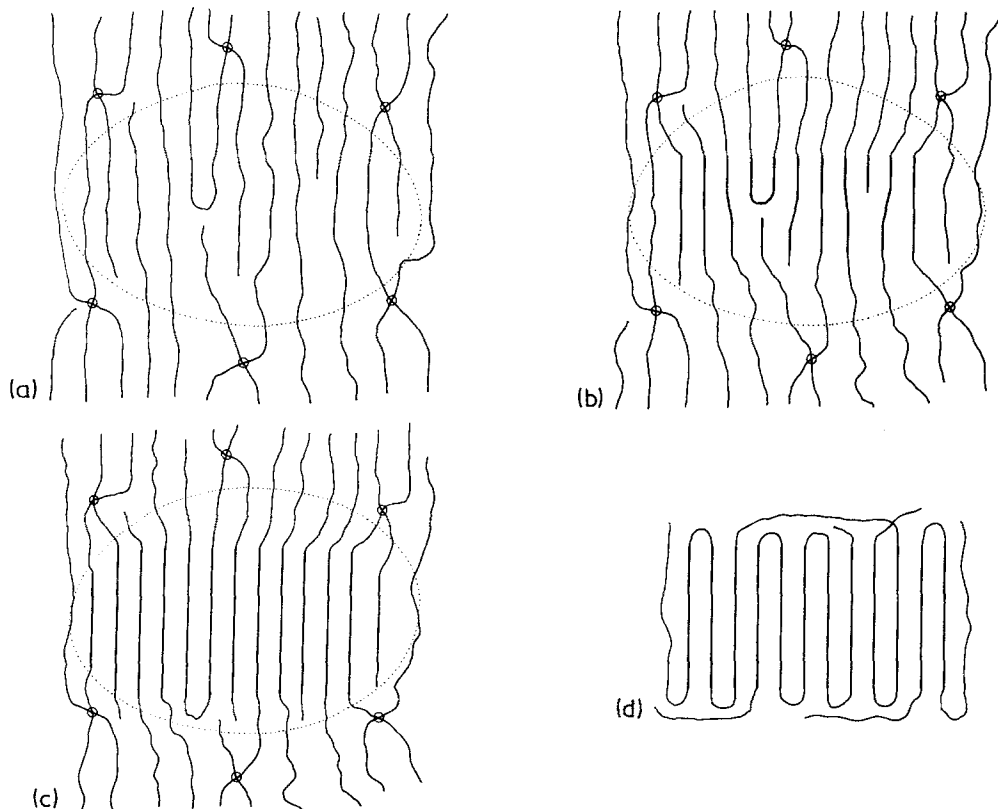

Figure 9 Morphology of the cold-stretched and annealed polypropylene. (The circles indicate mechanical tie-points). (a) Cold-stretched before crystallization; (b) micellar crystal; (c) recovery of a micellar crystal; (d) after transformation into a lamellar crystal.

investigation to define the influences of deformation mechanism and crystallization conditions on the formation of the micellar structure.

5. Summary

Polypropylene was drawn and annealed. The thermally-induced changes in microstructure were followed by SAXS, electron microscopy and diffraction, dynamical mechanical loss, and density. These results indicate the following model for the microstructure of the drawn material and for the phase transformation. The drawn material can be described as a very highly deformed crystal or paracrystal, with slight modulation of density in the draw direction. Upon low temperature annealing, the amplitude of the density modulation increases and the material develops a fringed micellar structure. After high temperature annealing, the material develops a distinct two-phase microstructure, with folded chain crystallites and distinct low-density amorphous domains.

Acknowledgement

References

1. K. HESS and H. KIESSIG, *Z. Phys. Chem.* **A193** (1944) 196
2. A. KELLER and A. O'CONNOR, *Nature* **180** (1957) 1289.
3. W. O. STATTON, *J. Polymer. Sci.* **41** (1959) 143.
4. R. BONART and R. HOSEMANN, *Makromol. Chem.* **39** (1960) 105.
5. *Idem, Kolloid Z. u. Z. Polymer* **186** (1962) 16.
6. A. PETERLIN, *J. Polymer Sci.* **C9** (1965) 61.
7. A. J. PENNINGS, *ibid.* **C16** (1967) 1799.
8. A. KELLER and M. J. MACHIN, *J. Macromol. Sci. Phys.* **1** (1967) 41.
9. E. W. FISCHER and H. GODDAR, *J. Polymer Sci.* **C16** (1969) 4405.
10. D. KRUEGER and G. S. Y. YEH, *J. Macromol. Sci. Phys.* **6** (1972) 431.
11. T. NAGASAWA and Y. SHINOMURA, *J. Polymer Sci. Phys.* **12** (1974) 2291.
12. J. PETERMANN and H. GLEITER, *Phil. Mag.* **31** (1975) 929.
13. K. H. ILLERS, *Kolloid Z. u. Z. Polymer* **231** (1969) 622.
14. P. J. FLORY, *J. Chem. Phys.* **15** (1947) 397.
15. A. PETERLIN, *J. Mater. Sci.* **6** (1971) 490.
16. J. H. SOUTHERN and R. S. PORTER, *J. Macromol. Sci.* **B4** (1970) 541.
17. G. CAPPACIO and I. M. WARD, *Polymer* **16** (1975) 239.
18. Z. MENCIK, *Chem. prumysl.* **10** (1967) 377.
19. P. J. FLORY, *J. Amer. Chem. Soc.* **84** (1962) 2857.
20. G. NATTA, P. CORRADINI and M. CESARI, *Atti. Accad. Nazl. Lincei* **21** (1956) 365.
21. R. L. MILLER, *Polymer* **1** (1960) 135.
22. A. KELLER, *Progr. Phys.* **31** (1968) 623.
23. M. DOLE, *Kolloid Z. u. Z. Polymer* **165** (1959) 40.
24. H. G. ZACHMANN, *Kolloid Z. u. Z. Polymer* **165** (1959).
25. E. W. FISCHER and S. FAKIROV, *J. Mater. Sci.* **11** (1976) 11047.
26. P. H. HERMANS and A. WEIDINGER, *Makromol. Chem.* **39** (1960) 67.
27. F. J. BALTA CALLEJA and A. PETERLIN, *J. Macromol. Sci. Phys.* **B4** (1970) 519.
28. G. S. Y. YEH and P. H. GEIL, *J. Macromol. Sci. Phys.* **B1** (1967) 251.
29. G. S. Y. YEH and S. L. LAMBERT, *J. Appl Phys.* **42** (1971) 4614.